EPJ Web of Conferences **302**, 08001 (2024) https://doi.org/10.1051/epjconf/202430208001
SNA + MC 2024

Evaluation of memory-preserving models for particle transport in random media

Gerald Samba[1,*], *Nicolas* Charpentier[1,2], *Bogdan* Stepanovic[1,2], *Olivier* Soulard[1,2], and *Laetitia* Laguzet[1]

[1]CEA, DAM, DIF, F-91297 Arpajon, France
[2]Université Paris Saclay, CEA, LMCE, 91680 Bruyères-le-Châtel, France

Abstract. A shortcoming of the Levermore-Pomraning (LP) model is its inaccuracy to treat the transport of particles in a diffusive material alternating with a transparent one. Enhanced-memory LP models have been proposed by Zimermann et al. (1991) and Larmier (2018) to circumvent this issue. The main purpose of this paper is to evaluate the PBS2 model also known as Algorithm C in these geometries. A second objective is to generalize it to an arbitrary number of interfaces allowing the same code to give either an approximation of the solution with a few interfaces or a reference result by increasing their number. A third one is to give a mathematical formulation of these models.

1 Introduction

The transport of particles in stochastic media has been studied since the 80's starting with the early work of Levermore and Pomraning [6]. These studies are driven by the need to describe the transport of neutrons in geometries where the location of the materials is not known exactly but only statistically, for instance in pebble-core reactors, in the corium in accidental situations, in cloudy atmospheres or in mixtures occuring in Inertial-Confinement-Fusion experiments [2]. When the dimensions of the heterogeneities are small compared to the distance of collisions, the simple atomic mix approximation may be used which only requires to weight the cross sections by the mean concentrations of each material. However in other situations, this approximation is no longer valid. To treat the transport in binary Markovian statistically mixed media, Pomraning proposed a model since named Levermore-Pomraning (LP) model [6]. Its unknowns are the ensemble-averaged fluxes in the two materials, solutions of two equations. Unfortunately, this model may be inaccurate in presence of scattering. Since then, models have been proposed to improve the LP model. As an example, Pomraning [5] proposed a model with two more equations for the interface ensemble-averaged fluxes. More recently, enhanced-memory models have been proposed. They keep in memory fictitious collision points where materials are known [8] or a fixed number of crossed interfaces [2, 9] between materials. However, the second models have not been generalized to an arbitrary number of interfaces. They have been tested in a limited number of configurations not including an alternance of very diffusive and transparent materials and no equation has been given for them. These are the issues we want to address in this paper.

*e-mail: gerald.samba@cea.fr

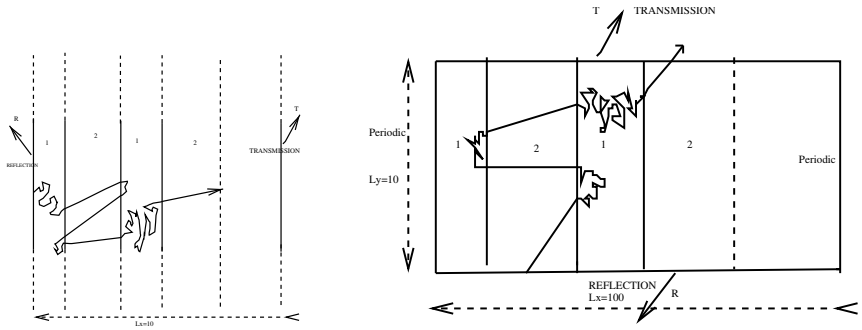

(a) 1D slab configuration (b) 2D configuration

Figure 1: The two configurations studied in this work

The remaining of this article unfolds as follows.

In section 2, definitions of interface and non-interface ensemble-averaged fluxes and exact equations are given which need some closure. In subsection 2.1, we recall the LP model. In subsection 2.2, we describe the PBS(n) model and give the equations verified by new ensemble-averaged fluxes. In particular, we demonstrate that this model may be seen as a truncation of an infinite system of equations. In section 3, we give numerical results for two configurations. The first is depicted in figure 1a, is very similar to those encountered in the published benchmarks 1D and stationary. The second much less studied, depicted in figure 1b, is 2D and unstationary.

2 Levermore-Pomraning models

In this study, the geometry is assumed to be statistically homogeneous, stationary, Markovian in the x direction, composed of two materials, hereafter referred to with the subscript $m \in 1, 2$. Because of the homogeneous hypothesis, the mean chord length Λ_m is independent of x. The Markovian hypothesis implies that the chord length $l(m)$ obeys the probability density function $f_m(l) = \dfrac{1}{\Lambda_m} \exp(-\dfrac{l}{\Lambda_m})$.

The concentration of the material m is given by $p_m = \dfrac{\Lambda_m}{\Lambda_1 + \Lambda_2}$. The transport is described by a one group linear equation with isotropic scattering. The cross sections are described by four constants $\sigma_{s,m}$ (scattering cross section) and $\sigma_{t,m}$ (total cross section).

In the 1D slab geometry, these models aim to calculate the ensemble-averaged fluxes, with the notations of [2], $\langle I(x,\mu)\rangle = \sum_{i=1}^{2} p_i \langle I^i(x,\mu)\rangle$ with $\langle I^m(x,\mu)\rangle = \dfrac{\int_{X_m(x)} \mathcal{P}(q) I^{(q)}(x,\mu) dq}{p_m}$, where $\mathcal{P}(q)$ is the probability of an occurrence of a realization q, X the ensemble of the realizations, $X_m(x) = \{q \in X | q(x) = m\}$ the subset of X such that the material at x is m, $p_m = \int_{X_m(x)} \mathcal{P}(q) dq$ the concentration of the material m and $I^{(q)}(x,\mu)$ the particle flux depending on x and μ the cosine of the direction with the x axis solution of the transport equation for one realization q:

$$\mu \partial_x I^{(q)}(x,\mu) + \sigma_t^{(q)}(x) I^{(q)}(x,\mu) = \frac{\sigma_s^{(q)}(x)}{2} \int_{-1}^{+1} I^{(q)}(x,\mu') d\mu'. \tag{1}$$

Multiplying the linear transport equation (1) by $\mathcal{P}(q)$ and integrating on $X_m(x)$, the exact equations in the 1D slab case verified by these ensemble-averaged fluxes are obtained:

$$\begin{aligned}\mu\partial_x(p_m\langle I^m(x,\mu)\rangle) + \sigma_{t,m}p_m\langle I^m(x,\mu)\rangle = \frac{\sigma_{s,m}}{2}\int_{-1}^{+1}(p_m\langle I^m(x,\mu')\rangle)d\mu' \\ +p_{\overline{m}\to m}(\mu)\langle I_{\overline{m}\to m}(x,\mu)\rangle - p_{m\to\overline{m}}(\mu)\langle I_{m\to\overline{m}}(x,\mu)\rangle.\end{aligned} \tag{2}$$

$\overline{m} = (m \bmod 2) + 1$ is equal to 2 for $m = 1$ and 1 for $m = 2$. Thus, equation (2) is valid for $m = 1$ and $m = 2$. The interface ensemble-averaged fluxes are:

$$\langle I_{m\to\overline{m}}(x,\mu)\rangle = \frac{\displaystyle\int_{X_{m\to\overline{m}}(x,\mu)}\mathcal{P}(q)|\mu|I^{(q)}(x,\mu)dq}{p_{m\to\overline{m}}(\mu)},$$

where $X_{m\to\overline{m}}(x,\mu)$ is the subset of realizations such that x is an interface between materials m and $\overline{m}$ and material m is at the left (resp. right) of the interface if μ is positive (resp. negative). In the case of 1D homogeneous Markovian mixtures, the probability $p_{m\to\overline{m}}$ per unit length is defined by:

$$p_{m\to\overline{m}}(\mu) = \int_{X_{m\to\overline{m}}(x,\mu)}|\mu|\mathcal{P}(q)dq = \frac{p_m|\mu|}{\Lambda_m}.$$

This leads to:

$$\mu\partial_x(p_m\langle I^m\rangle) + \sigma_{t,m}p_m\langle I^m\rangle = \frac{\sigma_{s,m}p_m}{2}\int_{-1}^{+1}\langle I^m(\mu')\rangle d\mu' + \frac{|\mu|p_{\overline{m}}}{\Lambda_{\overline{m}}}\langle I_{\overline{m}\to m}\rangle - \frac{|\mu|p_m}{\Lambda_m}\langle I_{m\to\overline{m}}\rangle. \tag{3}$$

The LP models approach the quantities $\langle I^m(x,\mu)\rangle$ and $\langle I_{m\to\overline{m}}(x,\mu)\rangle$. For example, Pomraning designed a closure named Interface model [5] composed of four equations verified by these four ensemble-averaged fluxes. But the simplest model, named in the following, standard LP model [1, 6] makes the approximation $\langle I_{m\to\overline{m}}\rangle = \langle I^m\rangle$.

2.1 LP standard model

The simulation of the standard LP model by a Monte-Carlo method is named Chord-Length-Sampling [9].

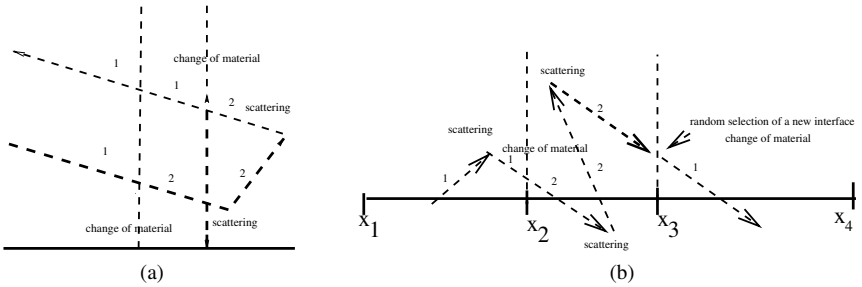

Figure 2: Typical trajectory with standard LP model (a) and LP model with memory (b)

The drawback of this model is that, after each scattering event, the particle forgets the last interface it has crossed. Thus, particles may encounter an unrealizable geometry during

their tracking as illustrated in figure 2a. In this situation, the particle first enters the material 2, goes through two collisions, then goes back in material 1. But, since the interface between the two materials is sampled at each scattering event, the interface has changed resulting in an unrealizable geometry.

This drawback does not exist if the materials are purely absorbing. The standard LP model is exact in this case as it was demonstrated in the pioneering works [3] on the LP model.

The enhanced-memory LP models, described in the following section, where particles retain some interfaces during their tracking alleviate this drawback. Retaining a sufficient number of cells during the tracking of a particle, as long as it stays in these cells from its birth to the exit of the domain prevents the situation illustrated in figure 2a. Thus, more accurate results may be obtained.

2.2 Enhanced-memory LP models

These models [2, 9] differ by the amount of geometry that the particles keep in memory during their tracking. They may retain one cell. This model is named PoissonBoxSampling1 [2] in 1D, 2D, 3D or Algorithm B in 1D [9]. They retain two cells in PBS2 [2] in 1D, 2D, 3D or Algorithm C in 1D [9].

These models are usually described by their implementation as a Monte-Carlo tracking but no equation, to our knowledge, is given. In this paper, we give, in the 1D slab case, with the boundary condition of the 1D test (figure 1a), the underlying equations of these models extended to an arbitrary n number of cells.

For that, we give some definitions, for $i \in 1, 2, ..., n$:

$\langle I_i^{m,x_1,x_2,.....,x_{n+1}}(x,\mu)\rangle = \frac{\int_{X^i_{m,x_1,x_2,.....,x_{n+1}}(x)} \mathcal{P}(q) I^{(q)}(x,\mu) dq}{p^i_{m,x_1,x_2,....,x_{n+1}}}$. $X^i_{m,x_1,x_2,.....,x_{n+1}}(x)$ is the subset of realizations such that x is in $[x_i, x_{i+1}]$, x_1, x_2, $...x_{n+1}$ are interfaces between materials, $[x_1, x_2]$ is composed of material m, $[x_2, x_3]$ of material $\overline{m}$, $[x_i, x_{i+1}]$ of material m_i, ,....., $[x_n, x_{n+1}]$ is composed of material m_n. $\langle I_i^{m,x_1,x_2,.....,x_{n+1}}(x,\mu)\rangle$ is the average of I on this subset of realizations and $p^i_{m,x_1,x_2,.....,x_{n+1}} = f_m(x_1, x_2).....f_{m_i}(x_i, x)p_{m_i}f_{m_i}(x, x_{i+1})....f_{m_n}(x_n, x_{n+1})$ the probability of such realizations per $dx_1...dx_{n+1}$ with $f_m(x,y) = \frac{1}{\Lambda_m} exp(-\frac{|x-y|}{\Lambda_m})$.

From these ensemble-averaged fluxes with $n+1$ interfaces, we can derive the ensemble-averaged fluxes with $n, n-1, ..., 2$ interfaces, for instance to go from 3 to 2 interfaces,

$$\langle I^{m,x_1,x_2}(x,\mu)\rangle = \int_{x_2}^{L_x} dx_3 f_{\overline{m}}(x_3, x_2)\langle I_1^{m,x_1,x_2,x_3}(x,\mu)\rangle + \langle I_1^{m,x_1,x_2,L_x}(x,\mu)\rangle(1 - \int_{x_2}^{L_x} dx_3 f_{\overline{m}}(x_3, x_2))$$
$$+ \int_0^{x_1} dx_0 f_{\overline{m}}(x_0, x_1)\langle I_2^{\overline{m},x_0,x_1,x_2}(x,\mu)\rangle + \langle I_2^{\overline{m},0,x_1,x_2}(x,\mu)\rangle(1 - \int_0^{x_1} dx_0 f_{\overline{m}}(x_0, x_1)).$$

From this quantity, interface $I_{m\to\bar{m}}$ and non-interface ensemble-averaged I^m verifying the equation (3) may be calculated. The goal is now to approximate the quantities $\langle I_i^{m,x_1,x_2,.....,x_{n+1}}\rangle$ which give access to all quantities we are interested in. LP models with n cells in memory deal with this quantity. In the tracking of the particle, the particle retains in memory $n+1$ interfaces x_1, x_2,.. x_{n+1} and as long as it has not escaped from the interval $[x_1, x_{n+1}]$ no sampling of material is done (see figure 2b for $n = 2$).

The equation for $\langle I_i^{m,x_1,x_2,.....,x_{n+1}}(x,\mu)\rangle$, $x \in [x_i, x_{i+1}]$ writes as:

$$\mu\partial_x\langle I_i^{m,x_1,x_2,....,x_{n+1}}(x,\mu)\rangle + \sigma_{t,m_i}\langle I_i^{m,x_1,x_2,....,x_{n+1}}(x,\mu)\rangle = \frac{1}{2}\sigma_{s,m_i}\int_{-1}^{+1}\langle I_i^{m,x_1,x_2,....,x_{n+1}}(x,\mu')\rangle d\mu', \tag{4}$$

with boundary conditions for $i \in \{2, 3, ..., n-1\}$:

$$\langle I_i^{m,x_1,x_2,....,x_{n+1}}(x_i,\mu)\rangle = \langle I_{i-1}^{m,x_1,x_2,....,x_{n+1}}(x_i,\mu)\rangle \text{ for } \mu > 0.$$
$$\langle I_i^{m,x_1,x_2,....,x_{n+1}}(x_{i+1},\mu)\rangle = \langle I_{i+1}^{m,x_1,x_2,....,x_{n+1}}(x_{i+1},\mu)\rangle \text{ for } \mu < 0,$$

$$\text{for } i=1, \langle I_1^{m,x_1,x_2,....,x_{n+1}}(x_2,\mu)\rangle = \int_{x_{n+1}}^{L_x} dx_{n+2} f_{\overline{m}_n}(x_{n+1},x_{n+2})\langle I_1^{\overline{m},x_2,x_3,.....,x_{n+2}}(x_2,\mu)\rangle$$
$$+\langle I_1^{\overline{m},x_2,x_3,.....,L_x}(x_2,\mu)\rangle(1-\int_{x_{n+1}}^{L_x} dx_{n+2} f_{\overline{m}_n}(x_{n+1},x_{n+2})) + \langle I_2^{m,x_1,x_2,....,x_{n+1}}(x_2,\mu)\rangle \text{ for } \mu < 0, \tag{5}$$

$$\langle I_1^{m,x_1,x_2,....,x_{n+1}}(x_1,\mu)\rangle = 0 \text{ if } x_1 \neq 0 \text{ (or 2 if } x_1 = 0), \text{ for } \mu > 0,$$

$$\text{for } i=n, \langle I_n^{m,x_1,x_2,....,x_{n+1}}(x_n,\mu)\rangle = \int_0^{x_1} dx_0 f_{\overline{m}}(x_0,x_1)\langle I_n^{\overline{m},x_0,x_1,.....,x_n}(x_n,\mu)\rangle$$
$$+\langle I_n^{\overline{m},0,x_1,.....,x_n}(x_n,\mu)\rangle(1-\int_0^{x_1} dx_0 f_{\overline{m}}(x_0,x_1)) + \langle I_{n-1}^{m,x_1,x_2,....,x_{n+1}}(x_n,\mu)\rangle \text{ for } \mu > 0, \tag{6}$$
$$\langle I_n^{m,x_1,x_2,....,x_{n+1}}(x_{n+1},\mu)\rangle = 0 \text{ for } \mu < 0.$$

Note the integral term at the right of the equality in (5) (and a similar term in (6)) which corresponds to particles with interfaces $x_2, x_3, ..., x_{n+2}$, material $\overline{m}$ between x_2 and x_3 coming from $[x_2, x_{n+2}]$ at x_2 and changing their parameters from $x_2, x_3, ..., x_{n+2}$ to $x_1, x_2, ..., x_{n+1}$, thus forgetting x_{n+2} which is equivalent to make the approximation $\langle I_2^{m,x_1,x_2,x_3,.....,x_{n+2}}(x_2,\mu)\rangle = \langle I_1^{\overline{m},x_2,x_3,...x_{n+2}}(x_2,\mu)\rangle$. If this hypothesis is not made, one gets an infinite hierarchy of equations. Such hierarchies are described in [7]. Retaining n cells in the memory of the particle means that this hierarchy is truncated. Equation (4) and its boundary conditions are the main results of this work. They express the solution of the n-cells memory model.

3 Results

In order to evaluate this n-cells memory model in a diffusive material alternating with a transparent one, we have ran two tests. The first is 1D and stationary, the second 2D and unstationary.

3.1 1D stationary case

These tests are similar to those presented in [2][1][4] but differ by the data. The slab length is $L_x = 10$ (figure 1a). The medium is Markovian with mean chord lengths $\Lambda_1 = 1$ and $\Lambda_2 = 2$. The material 1, $\sigma_{t,1} = 10$, $\sigma_{s,1} = 9.9$ is very diffusive (10 mean free paths in a mean

chord length, $\frac{\sigma_{s,1}}{\sigma_{t,1}} = 0.99$) and the material 2, $\sigma_{t,2} = 0.01$, $\sigma_{s,2} = 0$, purely absorbing and almost transparent. The boundary condition at $x = 0$ is $I(x, \mu) = 2$ for $\mu > 0$ corresponding to one particle entering with Lambert's law $\int_0^1 \mu(p_1\langle I^1(0,\mu)\rangle + p_2\langle I^2(0,\mu)\rangle)d\mu = 1$. The reference calculation was obtained by sampling 10000 geometries and for each, by making one transport calculation using linear Discontinuous Finite Elements. To discretize the angular variable, the interval $[-1, +1]$ is partitioned in 32 equi-intervals and to discretize the spatial variable, each material cell of the tessellation is partitioned in 10 subcells of equal size. With these discretizations, the deterministic calculations are converged. The atomic mix results are also deterministic. The Monte-Carlo calculations used for all the LP calculations are done with 10^7 particles. Figure 3a shows the angular-averaged flux for one realization. One can see the change between the transparent regions, where the solution is close to a constant, and the opaque regions, where the solution decreases.

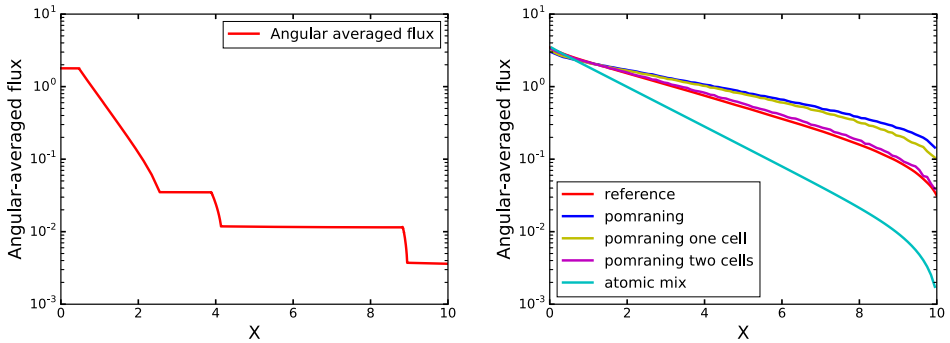

(a) (b)

Figure 3: Angular-averaged flux for a realization (a) and with different models (b)

In figure 3b and table 1, we compare the solutions of the LP standard model, the LP model with one cell in memory, the LP model with two cells in memory, the atomic mix model and the reference calculation. The standard LP model gives a smaller reflection. The LP models with one cell and two cells in memory improve this result. The atomic mix model for the reflection is accurate but fails for the transmission. The transmissions are too high for the standard LP model as well for the LP model with one cell in memory. The LP model result with two cells in memory is much better. The comparison of the profiles (figure 3b) of the angle-averaged fluxes confirms these results. For instance, the profile of the angle-averaged flux for the atomix mixed model is far below the reference one which results in a too much lower transmission.

3.2 2D unstationary case

In this test case, the geometry is a rectangle whose lengths are $L_x = 100$ and $L_y = 10$ (figure 1b). The materials are the same as in the 1D case. As this test is unstationary, we must set the speed of the particles which is fixed at 1. The materials 1 and 2 are parallel slots perpendicular to the x axis. The mean chord lengths are the same as in the 1D case. In this case, I depends on μ the cosine of the direction and ϕ the azimuth with the y axis. The boundary condition for $x = 0$ and $x = L_x$ is periodic : $I(L_x, y, t, \mu, \phi) = I(0, y, t, \mu, \phi)$, and for

Table 1: Comparison of the mean reflection and transmission values for the 1D stationary test case. Standard deviations are at least two orders of magnitude smaller than the corresponding mean values.

	Reflection	Transmission
Reference	0.7378	0.01838
Atomic mix	0.7784	0.00072
LP	0.5326	0.0752
LP one cell	0.6231	0.05466
LP two cells	0.7114	0.022

$y = 0$, at $t = 0$, a particle is launched with Lambert's law in angle and uniformly distributed on the segment $[0, L_x]$. This is obtained by setting $I(x, 0, t, \mu, \phi) = \delta(t)\frac{1}{\pi L_x}$ for $\mu > 0$ such that $\int_0^{Tmax} dt \int_0^{L_x} dx \int_0^1 \mu d\mu \int_0^{2\pi} d\phi(p_1\langle I^1(x, 0, t, \mu, \phi)\rangle + p_2\langle I^2(x, 0, t, \mu, \phi)\rangle) = 1$.

The reference results are obtained by sampling 100 geometries and for each geometry by making a Monte-Carlo calculation with 10^5 particles. The LP calculations are done with 10^7 particles.

Table 2: Comparison of the time-averaged mean reflection and transmission values for the 2D unstationary test case. Standard deviations are at least two orders of magnitude smaller than the corresponding mean values.

	Reflection	Transmission
Reference	0.496768	0.203714
LP	0.4587	0.1771
LP one cell	0.4828	0.1954
LP two cells	0.4917	0.2012

We observe the gain in accuracy with the LP two cells model in comparison with the standard LP model and the LP model with one cell. In this case (as opposed to the 1D case) the transmission is too low with the standard LP model (figure 4a) since the particles are too numerous in the diffusive material. It results in a too low transmission from material 2 and a larger transmission from the material 1 which can be seen in figure 4b. The profiles of the integrated (in angle, time and x) fluxes versus y in figures 6a, 5a and 5b are in agreement with the observed transmission. The LP model with one cell gives better results than the standard LP model (figure 6b). We have extended in the 2D case, the model to retain an arbitrary number of cells n. Retaining two cells in memory is sufficient to get reasonably good results as it can been seen in figures 7a, 7b. We observe the convergence of the LP models with memory towards the reference when n increases.

3.3 Explanation

In the following, we explain the better behaviour of the LP model with two cells in memory in the case of a succession of transparent and diffusive materials. In figure 8, a typical trajectory of a particle with the LP model with two cells in memory is drawn. The particle starts from A in the transparent material 2. At this stage, the particle knows three interfaces (shown on the

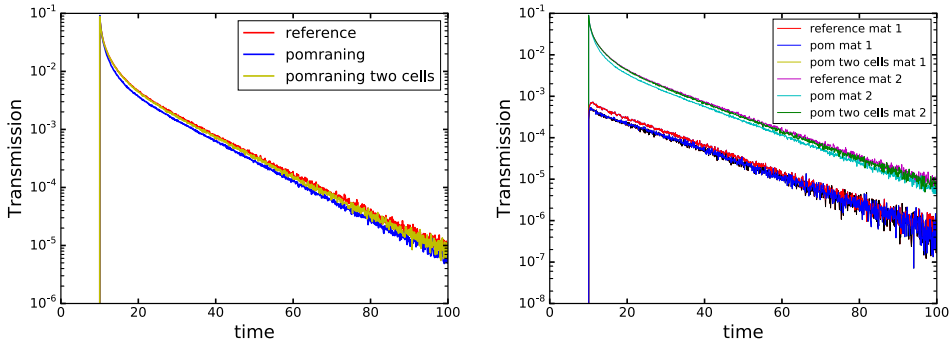

(a) (b)

Figure 4: Total transmission versus time (a) and from materials 1 and 2 (b)

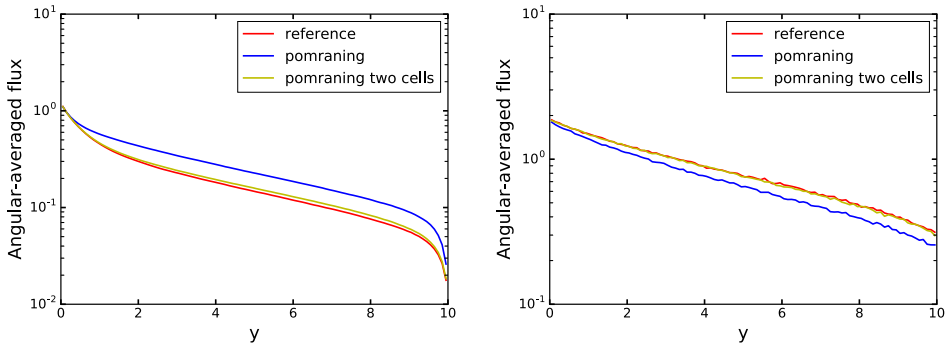

(a) (b)

Figure 5: $p_m < I^m >$ integrated in time, x and angle versus y for material 1 (a) and 2 (b)

figure), then enters in the diffusive material 1 at B, suffers scattering events then is transmitted in material 2 at C, crosses material 2, enters material 1 at D then goes back in material 2 at E and reenters material 1 at F. So far, the generated geometry is realizable but the interface at B was forgotten when the particle enters in material 1 at D so that when a new interface G is drawn, an unrealizability occurs between B and G .

But this situation is unlikely. We have computed by a Monte-Carlo method the probabilities of transmission, reflection, absorption in a slab of length 1 composed of material 1 with a Lambert's law for one particle at the boundary. We get $T = 0.0668$, $R = 0.784$ and $A = 0.149$. Then the probability of going twice through the diffusive medium is $0.067 \times 0.067 = 0.0044 < 1\%$ far less than the probability of a single transmission. This explains why the LP model with two cells in memory works better in such a geometry.

The probability of transmission through the diffusive medium may be approximated in the diffusion hypothesis by the formula $T_{diffusion} = \dfrac{2\gamma}{2\gamma cosh(2\gamma) + (\alpha+\beta)sinh(2\gamma)}$ with $\alpha = \dfrac{\sigma_{t,1}\sqrt{3}\Lambda_1}{2}$, $\beta = \dfrac{\sigma_{a,1}\sqrt{3}\Lambda_1}{2}$ and $\gamma = \alpha\beta$. For instance, in our case, it gives $T_{diffusion} = 0.0597$

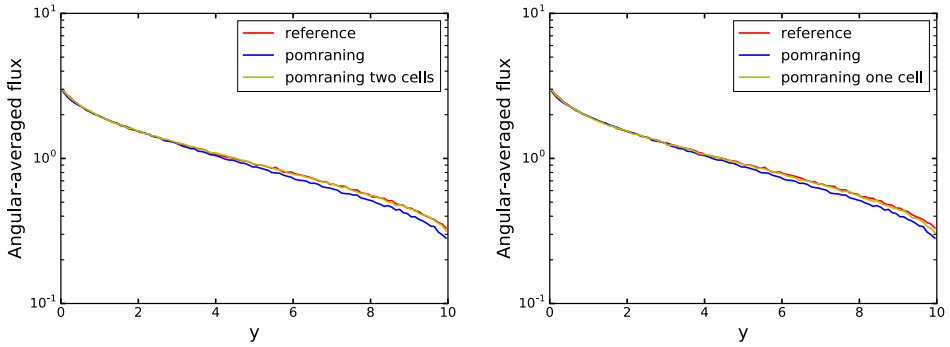

(a) (b)

Figure 6: Angular-averaged flux integrated in time, x and angle versus y, LP two cells (a) and LP one cell (b)

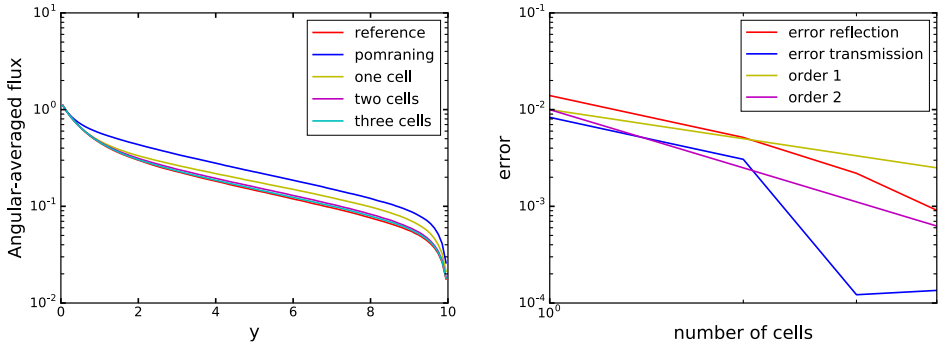

(a) (b)

Figure 7: $p_1\langle I^1\rangle$ integrated in time, x and angle versus y for material 1 (a) and error reflection, error transmission, versus the number of cells in memory (b)

instead of 0.0668. Therefore, a criterion to set the number of cells n to keep in memory could be $T^n_{diffusion} < \epsilon$ with an ϵ small enough.

Conclusion

In this work, we have established the equations of the LP model with two cells in memory called PBS2 or Algorithm C. So far, it had only been described by a Monte-Carlo algorithm. To this end was introduced new ensemble-averaged flux solutions of a truncated hierarchy of equations. The interface ensemble-averaged fluxes needed to close the LP equations are spatial moments of these quantities. This result was extended to an arbitrary number of interfaces.

Besides, we have shown why this model is superior to the standard LP model in the case of alternating transparent and diffusive media. Two geometries have been tested, the 1D slab

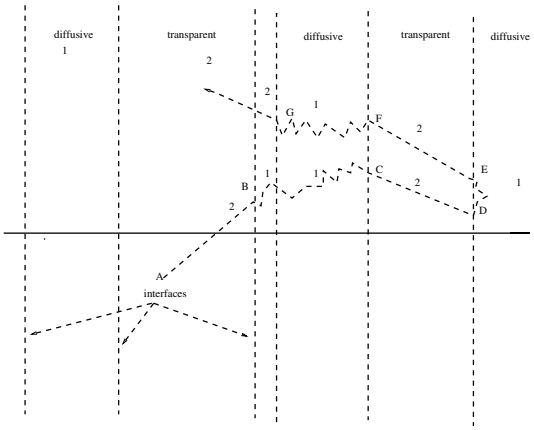

Figure 8: Trajectory with LP two cells model

geometry usually used in benchmark calculations and a 2D configuration never tested to our knowledge. Reflection, transmission, flux profiles were compared with the different models.

In the second test case, we have generalized the method by keeping n cells in memory with $n > 2$. We showed that the solution tends to the exact one by increasing n.

As a perspective, we intend to extend the PBS2 model in 3D to n interfaces. The corresponding method converges towards the Box Sampling results which can themselves be made very close to the general Markovian results [2] by multiplying the chord lengths by a constant. We are also interested in these methods to solve the system of equations with a participating medium which leads to a second equation for the temperature.

References

[1] Pomraning G.C Adams M.L, Larsen E.W. Benchmark results for particle transport in a binary markov statistical medium. *J. Quant. Spectros. Radiat. Trans.*, 42:253–266, 1989.

[2] Larmier C. *Stochastic particle transport in disordered media : beyond the Boltzmann equation.* PhD thesis, Université Paris-Saclay, October 2018.

[3] Vanderhaegen D. Radiative transfer in statistically heterogeneous mixtures. *J. Quant. Spectros. Radiat. Trans.*, 36:557, 1986.

[4] Larsen E.W. Davis I.M, Palmer T.S. A comparison of binary stochastic media transport models in solid-void mixtures. In *PHYSOR 2004 - The Physics of Fuel Cycles and Advance Nuclear Systems: Global Developments, Chicago*. 2004.

[5] Pomraning G.C. A model for interface intensities in stochastic particle transport. *J. Quant. Spectros. Radiat. Trans.*, 46:221–236, 1991.

[6] Gerald C. Pomraning. *Linear kinetic theory and particle transport in stochastic mixtures.* Singapore etc.: World Scientific, 1991.

[7] Sanchez R. Linear kinetic theory in stochastic media. *J.Math.Phys*, 30:2498, 1989.

[8] Olson A.J Vu E.H. Conditional point sampling: A stochastic media transport algorithm with full geometric sampling memory. *J. Quant. Spectros. Radiat. Trans.*, 272, 2021.

[9] Adams M.L Zimmerman G.B. Algorithms for monte carlo particle transport in binary statistical mixtures. *Trans. Am. Nucl. Soc*, 66:287, 1991.